ACS APPLIED MATERIALS & INTERFACES

www.acsami.org

Research Article

Multimodal Deformation of Liquid Metal Multimaterial Composites as Stretchable, Dielectric Materials for Capacitive Pressure Sensing

Elizabeth Bury and Amanda S. Koh*

Cite This: https://doi.org/10.1021/acsami.1c21734

Read Online

ACCESS | Metrics & More | Article Recommendations | Supporting Information

ABSTRACT: Traditional electronic devices are composed of rigid materials and components that tend to be unsuitable for soft robotic and stretchable electronic applications, such as wearable or continuous pressure sensing. However, deformable materials have the potential to improve upon traditional devices through enhanced sensitivity and responsiveness, better conformability and biocompatibility at the human−machine interface, and greater durability. This work presents deformable composite materials composed of the gallium−indium−tin alloy galinstan (GaInSn) that combines the conductivity of a metal and the intrinsic deformability of a liquid. Dispersing galinstan in an elastomer allows for the formation of deformable dielectric materials that have tunable mechanical and electrical behavior, for example, modulus and relative permittivity. Galinstan composites have been shown previously to have a minimal modulus impact on the elastomer but concurrently achieve impressive dielectric performance. However, galinstan dispersions can be costly and face challenges of mechanical and electrical reliability. Thereby, this work investigates multimaterial composites composed of galinstan and a rigid filler, either iron or barium titanate, with respect to morphology, mechanical behavior, dielectric behavior, and pressure sensing performance for the purpose of achieving a balance between a low modulus and superior electrical performance. By combining galinstan and rigid fillers, it was found that the mechanical and electrical properties, such as modulus, permittivity, loss behavior, sensitivity, and linearity of the multimaterial composites can be improved by tuning filler formulation. This suggests that these dielectric materials can be used for sensing applications that can be precisely calibrated to specific material properties and the needs of the user. These deformable multimaterial composites, found to be stretchable and highly responsive in sensing applications, will expand the current mechanical abilities of deformable dielectric materials to improve soft robotic and stretchable electronic devices.

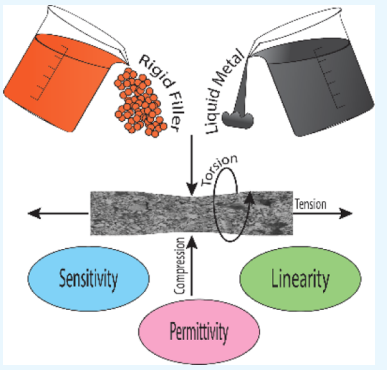

KEYWORDS: *liquid metal, dielectric permittivity, microcapacitor, deformable electronics, multimaterial composite, capacitive pressure sensing*

1. INTRODUCTION

Current electronic devices can oftentimes be rigid and bulky and have limited lifetimes, making them nonideal for applications that require device flexibility and longevity. To overcome these shortcomings, the field of stretchable electronics has emerged as an exciting alternative that combines deformable mechanical behavior with high performing technology to expand the current capabilities and applications of electronics. Soft and stretchable polymers (elastomers), such as polydimethylsiloxane (PDMS), are utilized as a common method to increase the mechanical robustness of electronics through stretchability, deformability, and conformability for such material applications.[1−4] However, elastomers typically exhibit poor electrical behavior that fall short of the required performance needed to match or improve on current electronics.[5−8] To improve elastomer electrical behavior, filler materials such as barium titanate[9−11] ($BaTiO_3$) and iron[12−14] have shown promising results in improving dielectric behavior, conductivity, and magnetization, respectively.

Composite materials that primarily rely on solid metallic or ceramic fillers to contribute the majority of the electrical performance, however, result in rigid and brittle composites that crack easily.[15,16] This behavior can be attributed to the modulus mismatch between the solid, rigid filler and the polymer matrix of the composite, which is clearly demonstrated by an increase in modulus as the concentration of rigid filler increases.[15−17] Additionally, mechanical behavior erodes as the composite approaches the maximum packing fraction, which is coupled to further degradation of the electrical properties of the composite.[16−18] Limitations such as these pose challenges for composite materials that rely solely on

Received: November 9, 2021
Accepted: February 25, 2022

solid metallic materials to achieve the needed electrical performance.

An alternative to utilizing rigid materials for stretchable electronic composites is gallium-based liquid metal alloys. These liquid metals, specifically the gallium-indium-tin alloy galinstan (GaInSn), are deformable, conductive fluids that can maintain their intrinsic electrical behavior, while undergoing deformation, which makes galinstan ideal for stretchable electronics and pressure sensing applications.[19−24] When dispersed into a polymer, the conductive bulk galinstan forms noncontinuous droplets within the polymer matrix, forming an insulating composite ideal for use as dielectric material in applications as pressure sensing.[25] Galinstan dispersions are beneficial compared to solid metallic materials due to a reduced impact on the bulk composite stiffness, elevated maximum loadings as compared to solid alternatives, and improved electrical performance during deformation.[26] While work has been done by adding rigid filler particles into galinstan itself,[27,28] little work, however, has been done trying to combine the benefits of the deformable liquid metal and high-performance rigid fillers into a polymer to take advantage of the best of both in a polymer composite. Specifically, multimaterial dispersions that decrease the amount of galinstan necessary to achieve both the desirable mechanical and electrical behavior.

Other published work on multimaterial dispersions has focused on solid materials and dispersion applications to achieve increased dielectric constants through functionalization,[29] composites for elastomer actuators,[30] and for hybrid elastomer gate dielectrics.[11] Alternatively, this work proposes multimaterial dispersions in PDMS composed of galinstan and either iron or barium titanate, which have not been previously studied. This novel blend of rigid, electrically active filler (either capacitive or conductive) enables composites with a previously unachievable balance of high electrical performance (i.e., high permittivity and ideal capacitive behavior) and mechanical performance (a modulus as close to the neat polymer as possible). The study that will be discussed here analyzes the fundamental components of mechanical deformation and capacitive output to detail how effects of the novel rigid/soft material blend. Iron was chosen because of its accessibility, high conductivity, and its potential usefulness for magnetic applications, while, on the other hand, barium titanate was chosen because of being a dielectric ceramic capable of dielectric constant values as high as 5000.[10] Through the addition of limited concentrations iron or barium titanate to galinstan dispersions, the multimaterial dispersions are expected to improve upon the electrical performance of galinstan-only dispersions by balancing the performance enhancement from the solid fillers, while still maintaining the desired stretchable mechanical behavior and to be useful for pressure sensing applications.

In this work, the morphology, deformation behavior, and electrical characteristics of galinstan-only, galinstan−iron, and galinstan−barium titanate multimaterial composites were analyzed to determine the result of combined rigid-liquid fillers. First, the multimaterial composites were interrogated mechanically with respect to their fluid properties and responses to torsional, tensile, and compressive deformation. The electrical behavior of the multimaterial composites was then investigated with respect to relative permittivity and phase angle, as well as resistance and impedance, as shown in Supporting Information. Lastly, their performance as a pressure sensor was evaluated by utilizing the analyzed fundamental mechanical and electrical behavior of these composites. The results of this work will allow for the evaluation of novel liquid metal multimaterial dispersions for use in sensing and an increased understanding of how to improve upon dielectric and stretchable electronic materials in order to potentially reduce the required amount of galinstan, increase the quality of the dielectric material, and decrease composite costs.

2. EXPERIMENTAL SECTION

2.1. Materials. Galinstan was purchased from RotoMetals (San Leandro, CA). Galinstan was used as purchased at a concentration of 68.5% Ga, 21.5% In, and 10% Sn. PDMS was purchased from Gelest, Inc. (Morrisville, PA). Molecular weights of vinyl-terminated PDMS and trimethyl-terminated PDMS were 62,700 g/mol (DMS-V41, 1×10^4 cSt) and 1250 g/mol (DMS-T11, 10 cSt), respectively. Commercial conductive iron powder (cubic crystal structure) consisted of irregularly shaped particles characterized through scanning electron microscopy (SEM) and X-ray diffraction (XRD) as shown in Supporting Information. Barium titanate ($BaTiO_3$, BTO) was purchased from Sigma-Aldrich (St. Louis, MO) and used as received. BTO (cubic crystal structure) was also characterized through SEM and XRD and consisted of roughly spherical shaped particles with a cubic crystal structure, the results of which can be found in Supporting Information. Composites were cured through mixing with a 800 ppm platinum−cyclovinylmethylsiloxane complex catalyst and tetrakis(dimethylsiloxy)silane cross-linker. The catalyst and cross-linker were also purchased from Gelest, Inc.

2.2. Forming Composites. All composites were formed using a 1:1 vol/vol blend of the vinyl-terminated (V41) and the trimethyl-terminated PDMS (T11). Composites were made with 0, 10, or 30 vol % of galinstan and 10, 20, or 30 vol % of the rigid filler (BTO or Fe). All composites were mixed using a Caframo (Ontario, Canada) High Torque Overhead Stirrer at 1800 rpm for 2 h. Two methods of composite preparation were used. For the first method (referred to herein as FM1), all components were added simultaneously and mixed as described previously. This was done for all BTO composites and for one set of Fe composites. The second method of preparation (referred to herein as FM2) involved first mixing the galinstan and PDMS blend for 1 h and 50 min at 1800 rpm, adding Fe to the blend, and subsequently mixing for another 10 min at 1800 rpm. Samples to be cured were subsequently blended with the catalyst and cross-linker, poured into Teflon molds, and kept at 82 °C for 72 h. During fabrication of all composites, the two materials, galinstan and either barium titanate or iron, were not intentionally alloyed together but rather were added into PDMS to form a composite as two discrete entities. No macroscopic phase separation or filler aggregation was observed between composite mixing and curing. All samples were made and tested in triplicate. All cured samples were free-standing and showed no change in morphology, either through filler settling or aggregation, during the time period of these experiments.

2.3. Mechanical Characterization. Composites were characterized in their cured state. The cured samples were characterized for their compressive, tensile, and torsional modulus. The composite torsional storage and loss modulus (G' and G'') were measured on the TA Instruments DHR-2 rheometer using a torsion rectangular fixture at 25 °C. Composite tensile modulus was measured on an Instron (Norwood, MA) Universal Mechanical Testing (UMT) apparatus using a 10 N load cell and rubber-faced grips. Composite compressive modulus was also measured on the Instron UMT using a 50 kN load cell and 2 in. diameter steel pressure platens. During the duration of these experiments, no hysteresis was observed.

2.4. Electrical Characterization. Composites were interrogated electrically (impedance, capacitance, dielectric loss, and phase angle: $|Z|$, C_p, D, θ) using a Keysight (Santa Rosa, CA) E4990A Impedance Analyzer with the 16451B Dielectric Test Fixture at frequencies from 500 Hz to 5 MHz. Capacitance and phase angle values were of primary importance to the work here. Resistance and impedance values can be found in Figures S3 and S4, respectively. Composite

https://doi.org/10.1021/acsami.1c21734
ACS Appl. Mater. Interfaces XXXX, XXX, XXX−XXX

samples were characterized only in the cured state. Composites were tested with thicknesses of 1 and 0.5 mm to remove error relating to the relative sizes of the filler as compared to the cured composite.

2.5. Microscopy Energy-Dispersive Spectrometry. Elemental analysis was performed using SEM and energy-dispersive X-ray spectroscopy (EDS) on cured composites of 30 vol % iron and barium titanate, respectively, for both 10 and 30 vol % galinstan using the Apreo FE-SEM of the Alabama Analytical Research Center (AARC) at The University of Alabama. The operating conditions were 20 kV accelerating voltage and 6.3 pA beam current.

2.6. Pressure Sensing. Cured composites were measured for pressure sensing through simultaneous electrical and compressive interrogation. Composites, 2 in. in diameter and 0.25 cm thick, were compressed at 0.13 mm/min on the Instron UMT, while being interrogated with the Keysight Impedance Analyzer. Two thin copper plates on either side of the composites were utilized as the parallel plates of a capacitive sensor in order to measure the electrical behavior during the compressive deformation. A scan of $|Z|$, C_p, D, and θ from 1 to 100 kHz was performed roughly five times per second. The electrical measurements were controlled automatically through a MATLAB script. Reported pressure sensitivity is taken from the linear regime of compressive force versus strain.

3. RESULTS AND DISCUSSION

3.1. Multimaterial Composite Morphology. Multimaterial composite morphology is essential to providing insights into the composite mechanical and electrical behavior to further understand the intended material applications. Unlike the rigid BTO and Fe (size and shape shown in Figure S2), the size and shape of the galinstan particles are dependent upon many factors, including viscosity of the galinstan dispersion, overall filler concentration, and amount of galinstan, as thoroughly investigated by Koh et al. where they detailed how these factors affect the "control group" in this paper of neat galinstan dispersions.[26] Additionally, with respect to the morphology behavior of the neat galinstan dispersions, it is known that the fluid shape of liquid fillers tends toward spherical particles; however, as more filler is added, the particles alter shape and jam together due to the packing of a liquid, which is known for a fluid emulsion, specifically the packing of high internal phase emulsions.[31−33] This behavior is observed for galinstan in the morphology of the multimaterial composites, but it is made more complex as the overall dispersion viscosity is also a function of the viscosity of the continuous phase and the galinstan/filler concentration. The morphologies of the 10BTO and 30BTO composites with 10GaInSn and 30GaInSn is shown in Figure 1. For the 10GaInSn BTO composites, the galinstan droplets appear similar in size to the barium titanate. For the 30GaInSn BTO composites, the galinstan droplets have a variety of sizes from those similar to that of barium titanate up to approximately 20× the size of the rigid filler, which demonstrates the polydispersity of galinstan dispersions that has been observed in a previous work.[26] This polydispersity may be due to inhomogeneous distribution of shear forces throughout the sample and is likely due to interaction between galinstan and barium titanate. Generally, the droplet size of galinstan decreases through shear mixing, but barium titanate particles may block the shear force from and cause increased galinstan polydispersity. It is not expected that additional mixing energy would improve the polydispersity as the dispersion was mixed for 2 h and is expected to have reached equilibrium.

The morphologies of the 10Fe and 30Fe composites with 10GaInSn or 30GaInSn for FM1 and FM2 are shown in Figure 2. For FM1, the iron and galinstan appear to be aggregated,

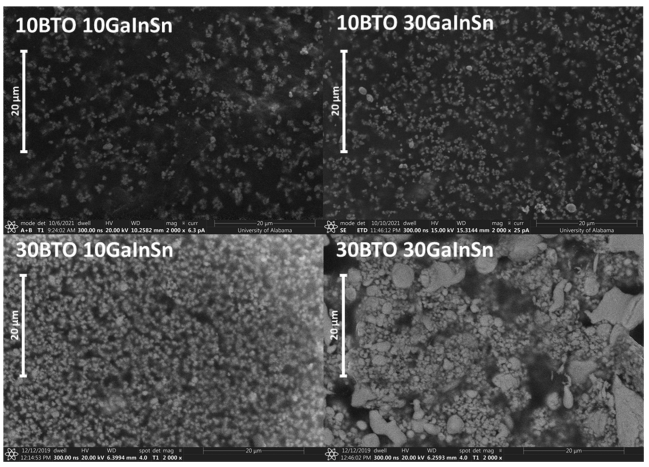

Figure 1. Morphology of the barium titanate composites. Row 1: 10BTO 10GaInSn and 10BTO 30GaInSn. Row 2: 30BTO 10GaInSn and 30BTO 30GaInSn. (from left to right) Scale bar size is 20 μm.

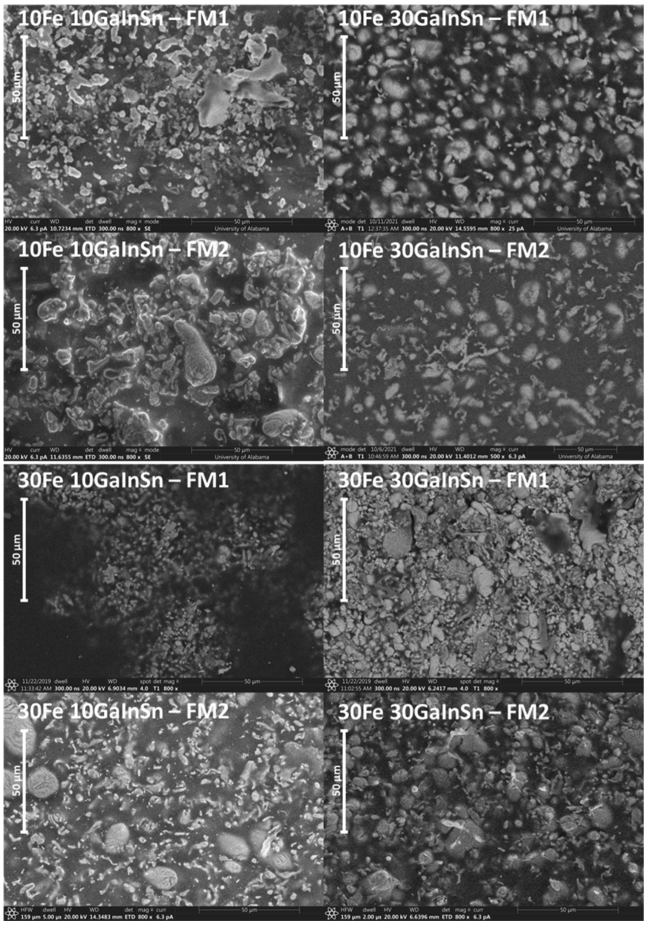

Figure 2. Morphology of the FM1 and FM2 iron composites. Row 1: 10Fe 10GaInSn−FM1 and 10Fe 30GaInSn−FM1. Row 2: 10Fe 10GaInSn−FM2 and 10Fe 30GaInSn−FM2. (from left to right) Row 3: 30Fe 10GaInSn−FM1 and 30Fe 30GaInSn−FM1. Row 4: 30Fe 10GaInSn−FM2 and 30Fe 30GaInSn−FM2. (from left to right) Scale bar size is 50 μm.

such that the iron particles are "coated" with galinstan droplets. The galinstan droplets in 10GaInSn 30Fe−FM1 composites appear overall smaller and more aggregated than in the 30GaInSn 30Fe−FM1. The smaller droplet size at 10GaInSn

https://doi.org/10.1021/acsami.1c21734
ACS Appl. Mater. Interfaces XXXX, XXX, XXX−XXX

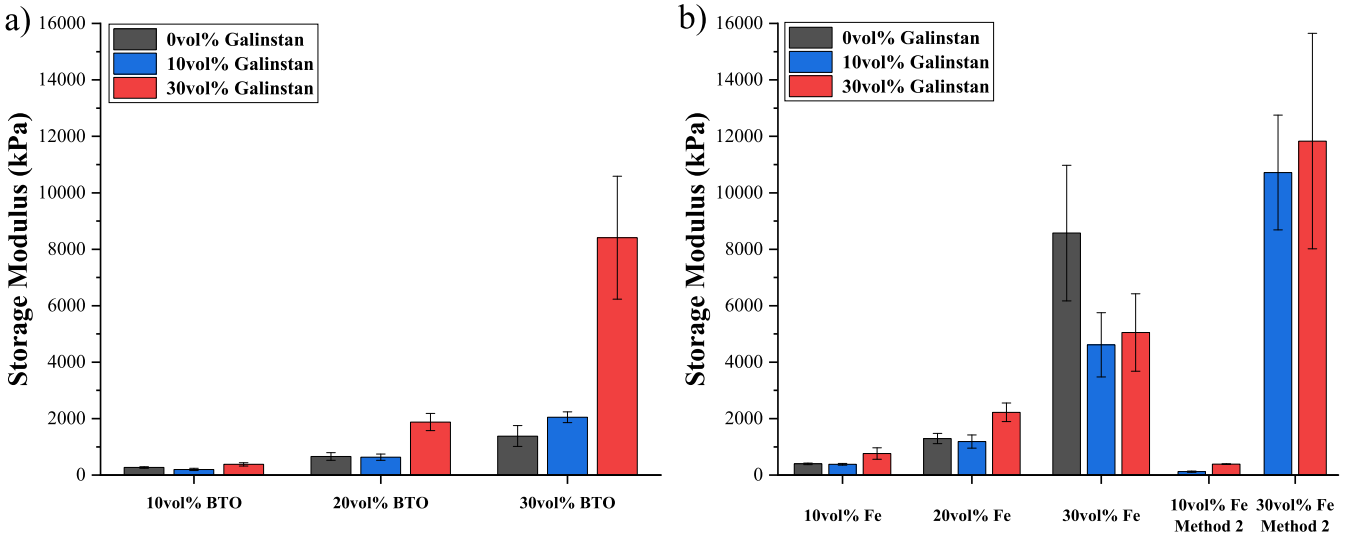

Figure 3. Torsion modulus behavior of the multimaterial composites at varying concentrations of (a) barium titanate and (b) iron with 0, 10, and 30 vol % of galinstan taken at 1 Hz and 0.1% strain.

than at 30GaInSn is most likely due to the iron blocking or impeding shear forces similar to what was observed for the barium titanate dispersions. 10Fe−FM1 composites appear to have similar galinstan droplet sizes at both 10GaInSn and 30GaInSn, which is expected, as a lower concentration of iron will hamper the distribution of shear throughout the sample less. Overall morphological observations for FM1 suggest that the iron has a dominant impact on the galinstan during the fabrication process, resulting in unexpected galinstan droplet conformation.

For FM2, iron and galinstan droplets appear to be discrete and less aggregated compared to FM1. The galinstan droplets for 30GaInSn 30Fe−FM2 appear smaller than 10GaInSn 30Fe−FM2, while for the 10Fe−FM2 composites, the galinstan droplets appear to be similar at both 10GaInSn and 30GaInSn. This may be due to 30GaInSn 30Fe−FM2 having an overall higher packing concentration resulting in a higher viscosity that leads to smaller galinstan droplet sizes, a trend which has been demonstrated previously.[26] This is different from the FM1 behavior. The differences in the morphology between FM1 and FM2 are likely due to a difference in the amount of time the iron and galinstan are mixed together to form the final composite, as detailed previously where iron and galinstan are mixed together for the full 2 h for FM1 composites but only mixed together for the last 10 min for FM2 composites. This is reflected in the fact that Fe−FM1 and barium titanate have a similar morphological behavior, which is different from Fe−FM2. All three components (PDMS, galinstan, and rigid filler) of Fe−FM1 and barium titanate composites are mixed together for the full 2 h, thus leading to greater interaction and longer time for the rigid filler to disrupt the rupturing of the galinstan droplets. This leads to the generation of more interface between the galinstan and rigid filler, in addition to the galinstan−PDMS and rigid filler−PDMS interfaces, resulting in greater likelihood for wetting, adsorption, and aggregation. For Fe−FM2, iron has a reduced influence on the galinstan due to a shorter mixing time (10 min) and is less of an impediment to the shear forces on the galinstan. Reduced mixing time and contact time, particularly with the preruptured galinstan droplets, also results in less interaction at the galinstan−iron interface and less aggregation.

3.2. Multimaterial Composite Response to Torsional Deformation. Many potential applications of the galinstan multimaterial composites apply torsional strain (i.e., bending and twisting) on the material, such as energy harvesting wearable devices,[34,35] curvature sensors,[22] and biosensors.[36] To evaluate these composites for these specific composite material applications, the torsion storage modulus was measured at 1 Hz and 0.1% strain, shown in Figure 3. The torsion behavior of the barium titanate composites with 0, 10, and 30 vol % galinstan is shown in Figure 3a. Increasing the amount of barium titanate increases the storage modulus, which agrees with what has previously been seen in literature for solid fillers.[15,16] For 10BTO and 20BTO composites, increasing the galinstan concentration from 0GaInSn to 10GaInSn has a negligible impact on the storage modulus. For 30BTO, increasing galinstan concentration to 10GaInSn, however, did increase the storage modulus by 1.5×. Further increasing the galinstan concentration to 30GaInSn caused a significant increase in the storage modulus of 1.9× for 10BTO and a greater increase of 4.1× for 30BTO. The reason for the observed torsion behavior is likely due to a combination of the native stiffness of the barium titanate composite and an upper packing threshold, after which adding galinstan increases the storage modulus. Below 30 vol % of the total filler, there is little impact of adding filler to the system. However, the storage modulus increases when increasing the composite formulation by adding galinstan beyond 30 vol % of the total filler, which appears to be a system-specific packing threshold. The greatest impact of the increasing filler content past this threshold is observed at 60 vol % total filler (30BTO 30GaInSn).

The torsion behavior of the iron composites with 0, 10, and 30 vol % galinstan is shown in Figure 3b. Similar to the barium titanate composites, the torsion modulus of iron composites increased with the increasing concentration of iron. For FM1, adding 10GaInSn for 10Fe and 20Fe composites had little to no impact on the storage modulus, which was also observed in the barium titanate composites. When increasing to 30GaInSn for 10Fe and 20Fe composites, however, the storage modulus was approximately double that of 0GaInSn and 10GaInSn. Unlike the lower concentrations of iron, for 30Fe composites, increasing the amount of galinstan from 0GaInSn to 10GaInSn

https://doi.org/10.1021/acsami.1c21734
ACS Appl. Mater. Interfaces XXXX, XXX, XXX−XXX

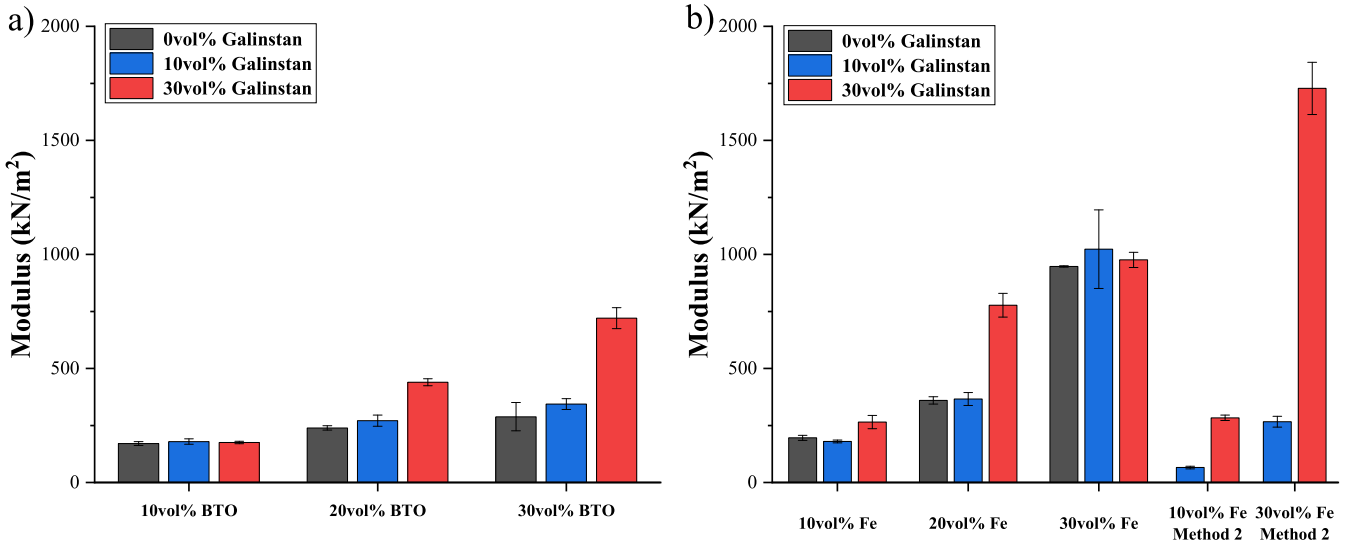

Figure 4. Tensile behavior of the multimaterial composites at varying concentrations of (a) barium titanate and (b) iron with 0, 10, and 30 vol % of galinstan.

decreased the torsion modulus, while the subsequent addition of galinstan to 30GaInSn had little effect. One possible reason for this decrease in modulus is a "lubricating" effect between iron particles originating from the liquid metal droplets that "coat" the iron particles. The aggregation, seen in SEM, reduces interparticle friction. For FM2, it was seen that for 10Fe, increasing the amount of galinstan to 10GaInSn initially shows a 3.3× decrease in the storage modulus, but a further increase of galinstan to 30GaInSn returns the storage modulus similar to the neat 10Fe composite. A different trend is seen at 30Fe−FM2 in which increasing the amount of galinstan consistently increases the storage modulus, although the increase is slight (1.3× and 1.4× increase for 10GaInSn and 30GaInSn, respectively, higher than neat 30Fe). This is likely due to reaching a packing threshold with FM2 that results in a continued increase in storage modulus, despite utilizing galinstan for packing concentrations past 30Fe.

It was also seen that increasing the amount of iron for FM2 has a greater impact on the storage modulus than FM1. The reason behind these observations may lie in the morphology difference between FM1 (aggregation of the galinstan and iron) and FM2 (discrete separation of the iron and galinstan), as seen in SEM. Based on these morphological differences, the reason FM2 has a higher storage modulus with the increasing galinstan concentration is expected to be because there is no lubricating effect seen with FM1, as there is less aggregation of the liquid metal and iron particles together. Therefore, the galinstan is predicted to move independently of the iron particles, resulting in a "jamming" of the particles and contribution to the increase in storage modulus.

Additionally, the torsion modulus of a 10BTO 10GaInSn composite is 3.3 times lower than that of a 20BTO composite, and a 20BTO 10GaInSn composite is 2.2 times lower than that of a 30BTO composite. Similarly, the torsion modulus of a 10Fe 10GaInSn composite is 3.4 and 10.8 times lower for FM1 and FM2, respectively, than that of a 20Fe composite, and a 20Fe 10GaInSn−FM1 composite is 7.2 times lower than that of a 30Fe composite. This demonstrates that the effect of galinstan replacing some solid filler actually lowers the storage modulus of the material despite the total composite having the same amount of the filler as a neat rigid filler composite. While galinstan is a liquid at room temperature, a previous work has demonstrated that galinstan cannot be treated as a standard liquid filler as it is not expected to depress the bulk material modulus when used on its own.[26] As such, the torsion modulus behavior described here is unique to multimaterial composites because the galinstan in the multimaterial composites acts more like a liquid filler by decreasing the torsion modulus of the neat rigid filler when used to replace a part of the total amount of the filler.

3.3. Multimaterial Composite Response to Tensile Deformation. Tensile strain, as described by the tensile modulus, is common to stretchable electronic material applications such as stretchable batteries,[37] device interconnects, composite fibers, and electrodes[38] in addition to physiological sensors.[36,39,40] The tensile modulus of the barium titanate composites with galinstan concentrations of 0, 10, and 30 vol % is shown in Figure 4a. For barium titanate composites, there was little to no impact on the tensile modulus when increasing galinstan concentration from 0GaInSn to 10GaInSn. However, further increasing to 30GaInSn resulted in a negligible change in tensile modulus for 10BTO and an increase in the tensile modulus of 1.6× and 2.1× for 20BTO and 30BTO, respectively. The reasoning behind this observed tensile behavior is similar to that of the observed torsion behavior, in that it is likely a result of both the native stiffness of the neat barium titanate composite and reaching an upper packing threshold results in restricted polymer deformation and an increase in tensile modulus. The large, expected increase in tensile modulus from galinstan is not observed here.[25] This is notable as it would be expected that the tensile modulus of a BTO−GaInSn dispersion would greatly increase with the increasing filler concentration because individually, as both galinstan[25] and barium titanate concentrations increase, the tensile modulus increases. For the iron composites, the tensile modulus of both methods of fabrication was tested and compared (Figure 4b). For 10Fe−FM1 and 30Fe−FM1, increasing the amount of galinstan had little impact on the rigidity of the multimaterial composite. These observations are substantially different for Fe−FM2 composites. Using FM2, increasing the galinstan concentration from 0GaInSn to 10GaInSn decreases the tensile modulus of the

https://doi.org/10.1021/acsami.1c21734
ACS Appl. Mater. Interfaces XXXX, XXX, XXX−XXX

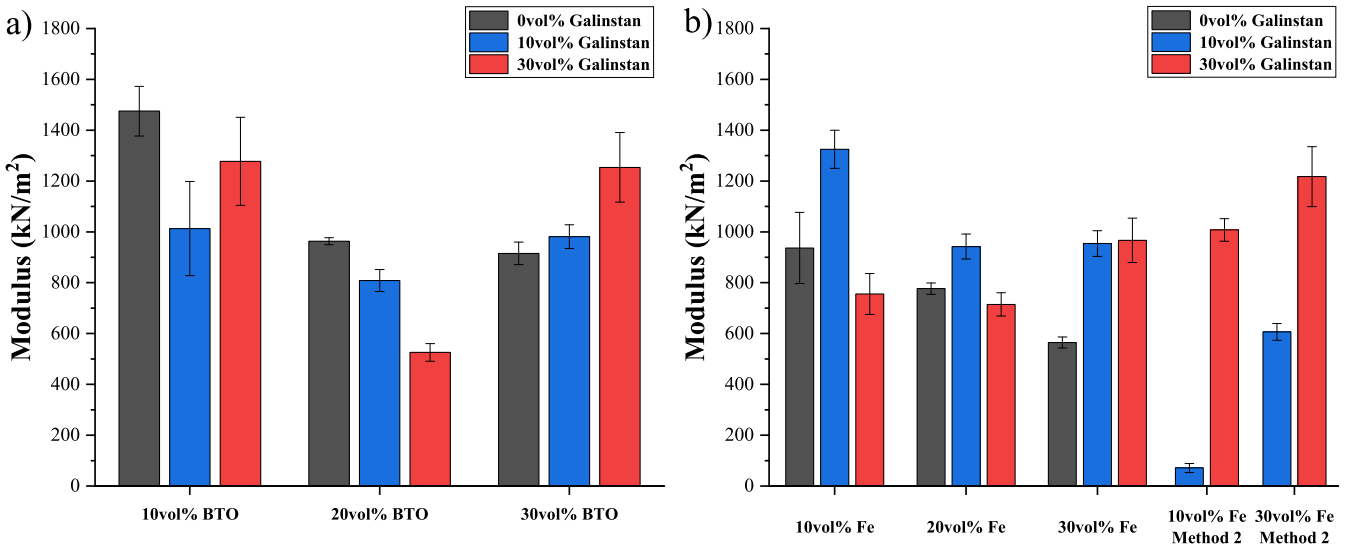

Figure 5. Compression behavior of the multimaterial composites at varying concentrations of (a) barium titanate and (b) iron with 0, 10, and 30 vol % of galinstan.

material by 3.0× and 3.5× for 10Fe and 30Fe, respectively. However, the tensile modulus increases by 4.3× and 6.5× for 10Fe and 30Fe, respectively, upon further increase in galinstan concentration from 10GaInSn to 30GaInSn.

Based on Figure 4, it is clear that modulus of the material is not solely a function of rigid filler or galinstan concentration. Other factors such as rigid filler size/shape, galinstan droplet size, filler/galinstan aggregation, and the interface between the fillers and PDMS as well as the fillers and galinstan (i.e., wetting) must also factor into the final tensile properties. For example, the tensile modulus decreases and then increases in iron composites with 10GaInSn and 30GaInSn, respectively, for FM2, which could be due in part to the elongation of galinstan in the cured PDMS "pockets". For FM2, galinstan and iron are discrete, and therefore, the galinstan deforms independently of the iron. At the lower concentration of galinstan (10GaInSn), the material demonstrates a lowered tensile modulus as the galinstan deforms in the cured "pockets" with the PDMS. However, with the increasing galinstan concentration to 30GaInSn, the galinstan concentration reaches a system-specific-packing threshold that results in an increased tensile modulus due to "jamming" of the elongated pockets of galinstan with the iron particles. Increasing the filler concentration, both of galinstan and iron, appears to have a larger impact on tensile modulus for FM2 than for FM1. The reason for the observed fabrication method dependence of the iron composite tensile modulus is likely due to the composite morphology. The iron and galinstan of FM1, as seen in SEM, are more aggregated than that of FM2 resulting in iron particles "coated" with liquid metal droplets. As a result, mechanical behavior of FM1 composites is solely dependent on the close proximity of the iron particles as a direct stress transfer from PDMS to iron is expected due to good PDMS/galinstan and galinstan/iron wetting. The tensile properties of FM2 composites, however, are due to a blend of the deformation of iron and galinstan independently.

In general, tensile modulus of the multimaterial composites was lower than the torsion modulus, which may be due to the effect that the type of deformation has on the filler particles, particularly galinstan. Galinstan, which is fluid, is locked into cured "pockets" in the PDMS. During torsional strain, a twisting motion is applied to the cured multimaterial composites. This torsional motion results in little to no deformation of the rigid particles and galinstan as the fillers are inside cured PDMS "pockets", and the majority of the deformation occurs in the bulk polymer. Increasing the concentration of the filler, however, causes "jamming" of the particles, which restricts the PDMS torsional deformation and leads to a higher modulus and stiffer material. Tensile testing, however, subjects the cured multimaterial composites to a different type of deformation, stretching through tensile strain. The stretching of the composites results in the elongation of the composite. The cured PDMS "pockets" of the galinstan in the multimaterial composites are elongated as it is stretched (rigid filler remains undeformed under tension). As galinstan is a liquid, it is expected that it will deform with the PDMS component of the multimaterial composite under tensile strain.

3.4. Multimaterial Composite Response to Compressive Deformation. Understanding how the multimaterial composites behave under compression is imperative as one of their primary material applications is for pressure sensing, which has been previously investigated using microchannels of liquid metal in a substrate[24,38] and dispersions of materials like carbon black or carbon nanotubes for capacitive pressure sensing.[41,42] The compressive modulus of the barium titanate composites with 0, 10, and 30 vol % galinstan is shown in Figure 5a. The impact of the increasing galinstan concentration differed based on barium titanate concentration. For 0GaInSn, when increasing the barium titanate concentration from 10BTO to 30BTO, there was a 1.6× decrease in compressive modulus. However, for 10GaInSn, there was little to no impact on the compressive modulus when increasing the barium titanate concentration from 10BTO to 30BTO. For 30GaInSn, there was a 2.4× decrease in compressive modulus from 10BTO to 20BTO that was recovered when the barium titanate concentration was further increased to 30BTO. One possible explanation for this compressive modulus behavior is poor wetting between the PDMS and barium titanate that is more prominent during compressive deformation. Poor wetting behavior leads to greater slip at the BTO/PDMS interface, which reduces the compressive modulus and results

https://doi.org/10.1021/acsami.1c21734
ACS Appl. Mater. Interfaces XXXX, XXX, XXX−XXX

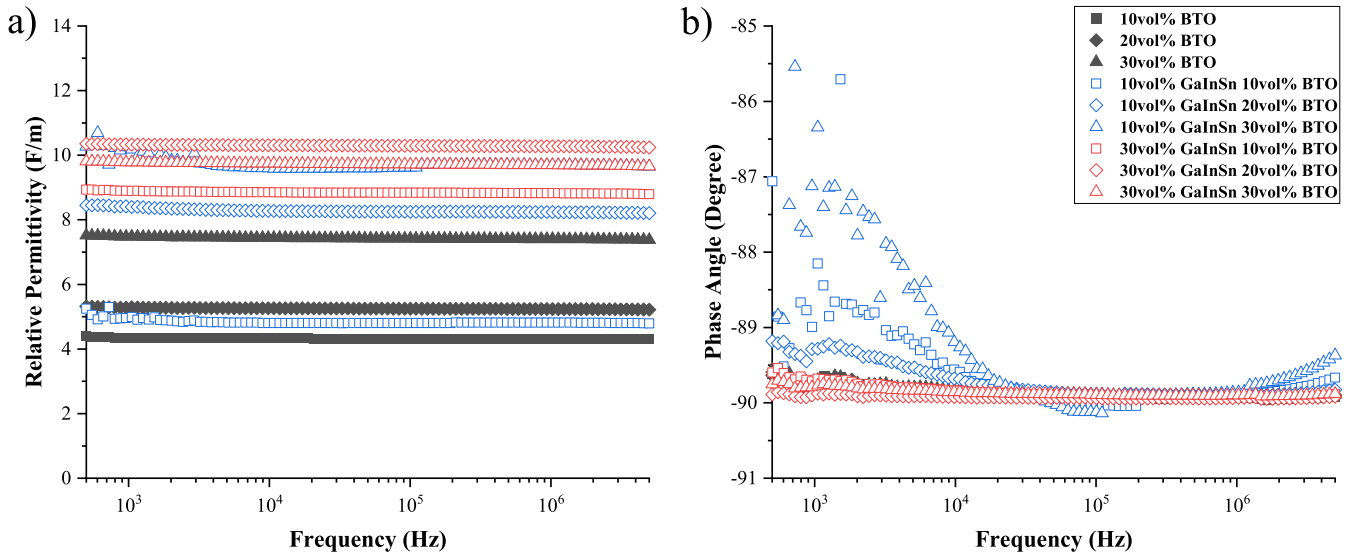

Figure 6. Frequency-dependent (a) relative permittivity and (b) phase angle at varying concentrations of barium titanate with 0, 10, and 30 vol % of galinstan. The same legend is used for both (a,b).

in the further reduction of compressive modulus with the increasing barium titanate concentration.[43]

For the iron composites shown in Figure 5b, there was an increase in compressive modulus when increasing the galinstan concentration to 10GaInSn for 10Fe−FM1 and 20Fe−FM1. Increasing the concentration further to 30GaInSn decreased the compressive modulus, so that it was similar to the neat iron composites for 10Fe−FM1 and 20Fe−FM1. For 30Fe−FM1, there was also an increase in compressive modulus upon increasing the galinstan concentration to 10GaInSn but increasing to 30GaInSn had no further impact on the compressive modulus. In the case of the FM2 iron composites, increasing the galinstan concentration increased the compressive modulus. For 10Fe−FM2, there was a 13.2× decrease in compressive modulus with the addition of 10GaInSn that returned to a compressive modulus slightly higher than neat 10Fe when the galinstan concentration was increased to 30GaInSn. For 30Fe−FM2, there was a minimal impact on the compressive modulus when increasing the galinstan concentration to 10GaInSn, unlike FM1, but a 2.2× larger compressive modulus than that of neat 30Fe−FM2 with 30GaInSn.

Results from Figure 5b demonstrate that, like BTO dispersions, the relationship between iron concentration, galinstan concentration, and compressive modulus is complex. While the compressive behavior of BTO and iron may have some similar root causes, differences are observed between FM1 and FM2 for iron specifically. When compressing a galinstan and PDMS composite, it is expected that galinstan will yield first, as the compressive modulus of galinstan (a liquid) is expected to be lower than the compressive modulus of PDMS (500 kN/m^2). For Fe−FM1 composites, liquid metal droplets form an interface between PDMS and iron due to aggregation. When the composite is compressed, the galinstan will deform first, but due to the close packing induced by aggregation the galinstan deformation is impeded, resulting in an increase in compressive modulus. As galinstan concentration further increases, however, the packing of galinstan becomes less dependent on the iron interface, and the galinstan deforms more readily. As the iron concentration increases, the overall filler concentration reaches the packing threshold, and this extra relaxation is impeded. For FM2, there is no induced close packing of the galinstan droplets due to aggregation, and the liquid metal can deform as discrete droplets, causing a drop in compressive modulus. Similarly, as the concentration of the overall filler increases, the compression of the liquid metal is once again restricted, and the compressive modulus increases.

Compared to the other kinds of mechanical deformation discussed in this work, the relationship between compressive behavior and composite formulation is highly complex. A greater complexity in compression rather than tension or shear has been previously seen in the literature with other composite systems.[44−46] One potential reason for the complexity that is shown by the galinstan multimaterial composites is that under compressive deformation the load is directly applied to the fillers, while for torsional and tensile deformation that force is largely experienced by the PDMS.

3.5. Electrical Characterization—Relative Permittivity and Phase Angle. The relative permittivity and phase angle of the multimaterial composites determine their effectiveness for dielectric material applications. Specifically, the higher the relative permittivity, the better the expected dielectric performance, and the phase angle describes the extent to which the dielectric can form an ideal capacitor. Previous work, utilized in this section to further understand the electrical behavior of these multimaterial composites, has extensively studied a microcapacitor model in dielectric composite materials, where the composite is evaluated as a network of microcapacitors that are randomly distributed in the host matrix.[47−51] The larger the area of the electrode "plate" (galinstan droplets in the BTO−GaInSn composites and galinstan and iron particles in the Fe−GaInSn composites), the higher the bulk capacitance, that is, the more microcapacitors the better the electrical performance. In addition to the overall composite dielectric behavior, there is also an observed frequency dependence for the electrical behavior of the iron−galinstan composites, while frequency independence is observed for the barium titanate−galinstan composites. This difference in observed electrical behavior based on composi-

https://doi.org/10.1021/acsami.1c21734
ACS Appl. Mater. Interfaces XXXX, XXX, XXX−XXX

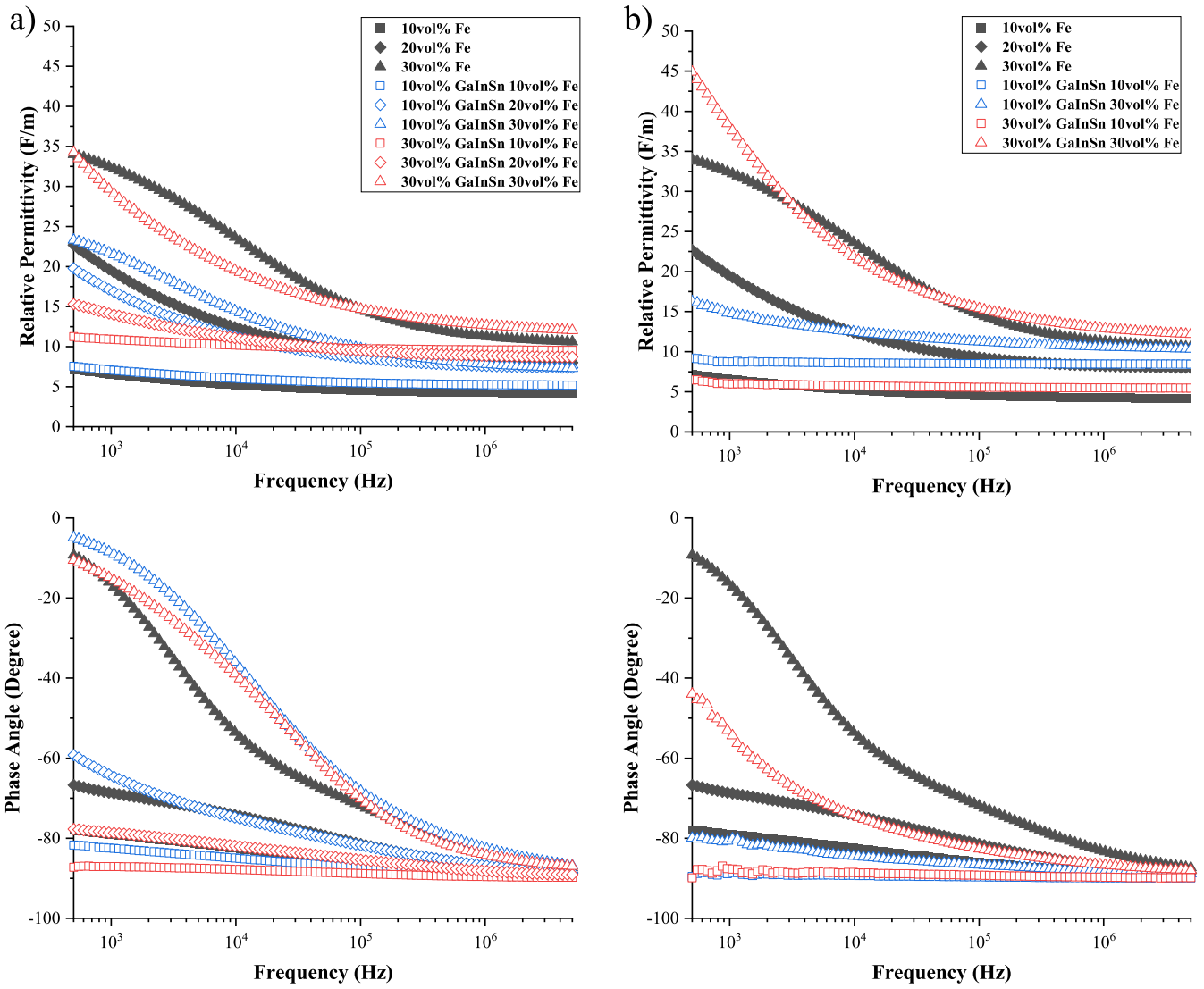

Figure 7. Frequency-dependent relative permittivity and phase angle at varying concentrations of iron for fabrication (a) Method 1 and (b) Method 2 with 0, 10, and 30 vol % of galinstan.

tion is not unique to these multimaterial composites. Previous work has found that neat iron composites exhibit frequency dependent behavior,[49] while neat barium titanate composites are generally frequency independent.[52]

The relative permittivity and phase angle of the barium titanate composites with galinstan concentrations of 0, 10, and 30 vol % are shown in Figure 6. The relative permittivity of the barium titanate composites increases with the increasing barium titanate concentration, as has been seen in other published works of barium titanate dispersions.[9,10] Increasing the galinstan concentration also increases permittivity, as expected.[26] The increase in relative permittivity due to the addition of galinstan is dependent on the barium titanate concentration. For example, at 10BTO, increasing from 0GaInSn to 10GaInSn and 30GaInSn increases the permittivity by 1.1× and 1.8×, respectively. At 30BTO, this increase is instead 1.3× and 1× (negligible increase). This suggests that the relative permittivity of the composite is dominated by the presence of barium titanate rather than the galinstan. Barium titanate has a high permittivity, and so, it is likely that the BTO permittivity overshadows the impact of the microcapacitors formed with the galinstan particularly at high BTO concentrations. The phase angles for the barium titanate composites with 0GaInSn and 30GaInSn are approximately −90°. The phase angle for composites with 10GaInSn had a greater frequency dependence than 0GaInSn or 30GaInSn but remain close to −90°. This suggests that the barium titanate and galinstan composites can form a good dielectric where the addition of galinstan does not increase lossy behavior.

The relative permittivity and phase angle of the iron multimaterial composites with 0, 10, and 30 vol % galinstan utilizing FM1 and FM2 are shown in Figure 7a,b, respectively. Increasing the iron concentration for both FM1 and FM2 increases the relative permittivity and results in a phase angle closer to zero. For 10Fe−FM1, increasing the galinstan concentration from 0GaInSn to 10GaInSn has little impact on the relative permittivity. This may be because galinstan droplets coat the iron particles, which disrupts iron conductive pathways. A larger increase in permittivity is observed from 10GaInSn to 30GaInSn as galinstan becomes the dominant microcapacitor electrode in the composite. For 20Fe−FM1, increasing the galinstan concentration has little effect on the relative permittivity from 0GaInSn to 30GaInSn. However, for 30Fe−FM1, the relative permittivity decreases from 0GaInSn

https://doi.org/10.1021/acsami.1c21734
ACS Appl. Mater. Interfaces XXXX, XXX, XXX−XXX

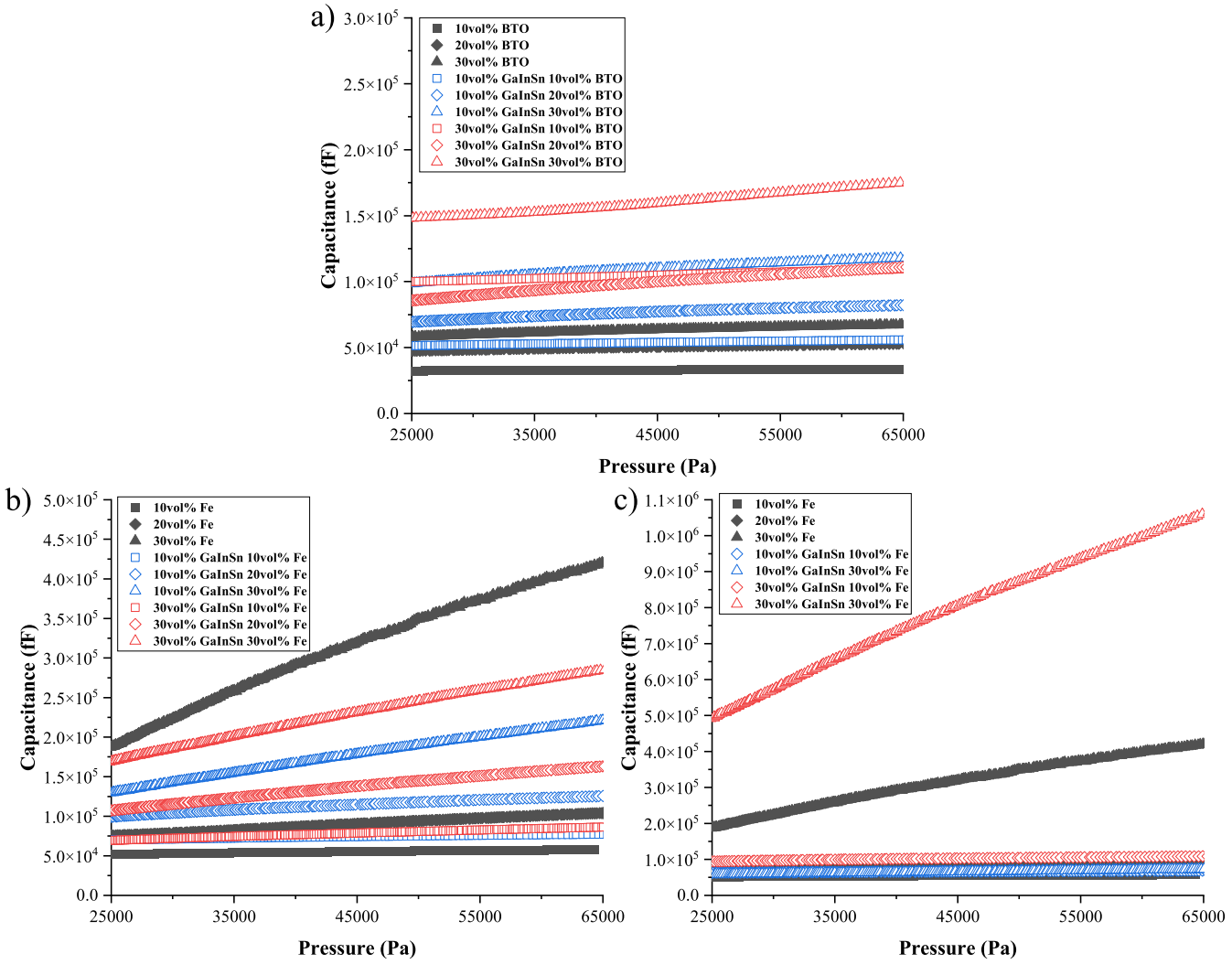

Figure 8. Capacitive response of the multimaterial composites under compression at varying concentrations of (a) barium titanate and for fabrication (b) Method 1 and (c) Method 2 for iron with 0, 10, and 30 vol % of galinstan. Note that the *y*-axis is different for each plot.

to 10GaInSn to that similar to neat 20Fe−FM1. This decrease in relative permittivity with the increasing galinstan concentration may be due to aggregation of the particles acting as one larger particle resulting in a decrease in the concentration of composite microcapacitors.[51] Upon further increasing the galinstan concentration to 30GaInSn, the relative permittivity increases to that similar of the neat 30Fe−FM1 composite.

For 10Fe−FM1, increasing the galinstan concentration resulted in the phase angle moving closer to −90°. For 20Fe−FM1, increasing the galinstan concentration either had a minimal effect or resulted in a phase angle closer to −90°. This demonstrates that coating the iron particles with galinstan droplets and disrupting the conductive pathways between the iron, the behavior that is seen for FM1 as galinstan concentration increases, results in reduced lossy behavior. As neat galinstan composites (see Supporting Information for 10GaInSn and 30GaInSn) have a phase angle closer to −90°, while neat iron composites have a phase angle closer to zero, the lossy behavior of the Fe−GaInSn composites is dominated by the galinstan, which agrees with the aggregated Fe−GaInSn microcapacitor model proposed here. However, for 30Fe−FM1, increasing the galinstan concentration has a minimal effect on phase angle, suggesting that increasing the iron concentration results in less effective disruption of the conductive pathways by galinstan.

With respect to FM2, for 10GaInSn−FM2 and 30GaInSn−FM2, increasing the iron concentration increases relative permittivity. Utilizing the microcapacitor model, this suggests that discrete particles form more microcapacitors overall and result in an increase in relative permittivity.[51] (See Supporting Information for 10GaInSn and 30GaInSn.) For 10GaInSn−FM2 and 30GaInSn−FM2, increasing the iron concentration results in the phase angle moving closer to zero. This further suggests that as the iron concentration is increased, the disruption of the conductive pathways by the galinstan is less effective.

4. LIQUID METAL COMPOSITE PRESSURE SENSING

To interrogate the galinstan multimaterial composites for pressure sensing applications, the composites were subjected to compressive loads up to 200−250 N, while simultaneously being monitored for capacitance. The bulk of previous work in liquid metal-based pressure sensors has focused on using deformable electrodes for capacitive sensors or conductive channels for resistance-based sensors.[20,43,53,54] Existing work on liquid metal composite dielectrics has demonstrated the

https://doi.org/10.1021/acsami.1c21734
ACS Appl. Mater. Interfaces XXXX, XXX, XXX−XXX

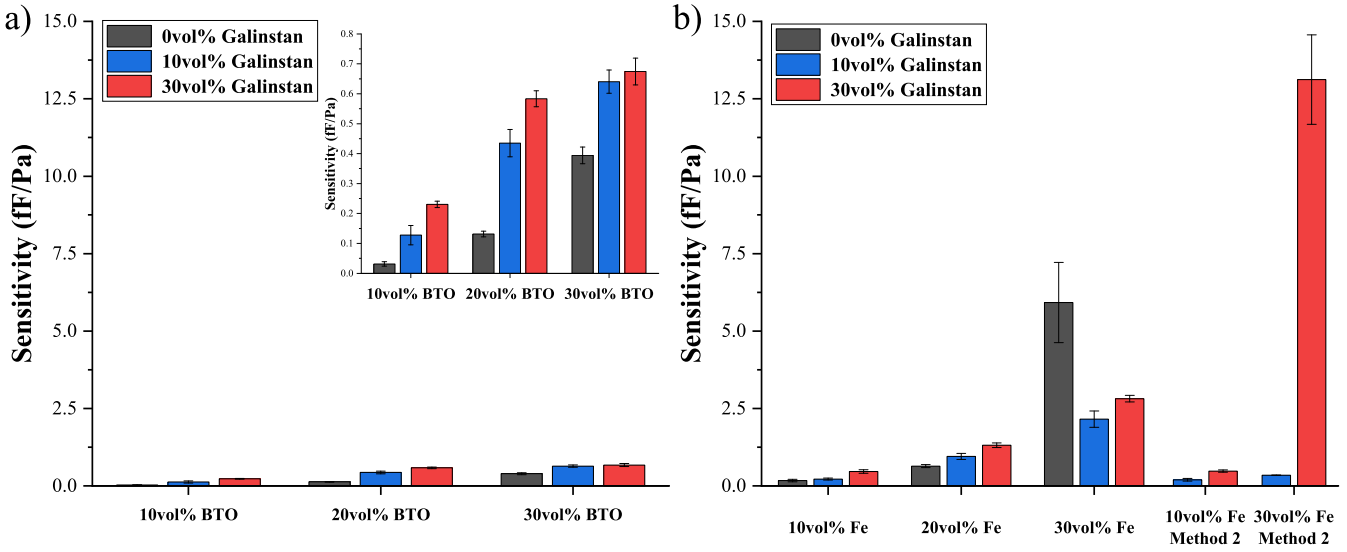

Figure 9. Sensitivity of the multimaterial composites under compression at varying concentrations of (a) barium titanate and (b) iron with 0, 10, and 30 vol % of galinstan.

durability and reliability of these materials and has indicated high sensitivity under tensile strain.[25,55−58] The capacitive response of the composites under compression is shown in Figure 8. To determine the sensitivity of the multimaterial composites under compression, the slope of change in capacitance with respect to pressure in the linear regime of the stress−strain response, described in Section 6, was analyzed and is shown in Figure 9. Sensitivity is described as the change in capacitance with respect to the added load (with units of fF/Pa). As expected, increasing the loading of conductive or capacitive filler generally increased the sensitivity of the material to pressure. This reflects the trend seen in Section 8 with respect to permittivity, as the material with higher permittivity is expected to have higher sensitivity. For BTO−GaInSn composites, the sensitivity of the multimaterial pressure sensor was largely independent of the composition of the sensor. This is seen with 20BTO as compared to 10G-10BTO, which have roughly the same sensitivity (0.13 fF/Pa), and 30 BTO as compared to 10G-20BTO, which also have roughly the same sensitivity (0.39 and 0.44 fF/Pa). Comparing the electrical and mechanical properties of these composites, each pair has similar permittivity values but not reliably the same compressive modulus. 20BTO and 10G-10BTO both have a compressive modulus of around 1000 kN/m^2 (964 and 1013 kN/m^2, respectively), while 30BTO has a modulus of 916 kN/m^2 and 10G-20BTO has a modulus of 809 kN/m^2. This suggests that for these low loss composites, the permittivity of the material is the dominant factor in the composite performance as a pressure sensor.

The fundamental trend of increasing the filler leading to increased sensitivity is also reflected in the Fe−GaInSn composites with the exception of 30Fe−FM1. When keeping the concentration of galinstan constant, increasing the iron loading consistently increased the material sensitivity (for both FM1 and FM2). For 30Fe−FM1, adding 10GaInSn to 30Fe reduced the sensitivity from 5.9 to 2.2 fF/Pa. Additional galinstan (30Fe 30GaInSn) had little effect on sensitivity. This trend was not observed for Fe−FM2, for which the addition of 10GaInSn to 30Fe showed a slight decrease in sensitivity, but a further addition of galinstan to 30GaInSn improved sensitivity dramatically to 13 fF/Pa. At 30Fe, neither trend is directly mirrored in the permittivity or compressive modulus data for the respective composites, demonstrating a more complex electromechanical response to compression for iron composites than BTO, which is especially sensitive to aggregation of the filler.

The multimaterial composite that had higher performance as a sensor when investigated with respect to sensitivity and change in permittivity with compression was the 30Fe 30GaInSn−FM2 composite. At the highest compressive strain measured, it had about double the change in permittivity than a previous work has measured with dielectric liquid metal elastomer foams.[59]

As the pressure sensing data presented suggest, the permittivity of a dielectric composite is one of the primary metrics that is used to assess potential future performance. This is based on the well-known expression for capacitance that relates dielectric permittivity, thickness, and area. The assumption that is made with this evaluation, as well as the basic interpretation of the stress−strain linear regime, is that permittivity remains constant when the material is deformed. This can be seen in most research that uses deformable dielectrics especially dielectric elastomeric actuators (DEAs). However, limited work, largely focused on the acrylic VHB, has demonstrated that dielectric permittivity can change with deformation. The exact mechanism that causes the change is not established, but there is clear evidence that under tensile strain, many elastomers show a reduction in permittivity. Kumar and Patra (2021) showed a reduction in dielectric permittivity from 5.67 to 2.89 when VHB was subjected to a 5× biaxial stretch.[60] Cohen et al. (2017) demonstrated a reduction in the dielectric permittivity of LDPE, HDPE, PTFE, and VHB 4910 under stretches of 2−4×.[61] More work has demonstrated that prestrain, commonly used to reduce electromechanical instability in DEAs, also changes dielectric permittivity. One potential explanation is that strain limits the ability of polymer chains to polarize with respect to an applied magnetic field as they become more constrained in movement. There is little work focused on the effect of deformation on filled polymer composites. Fujihara et al. (2019) demonstrated a reduction in permittivity from roughly 6.5 to 4.25 for 10 vol % TiO_2 in silicone.[62] Huang and Schadler (2017) showed a

https://doi.org/10.1021/acsami.1c21734
ACS Appl. Mater. Interfaces XXXX, XXX, XXX−XXX

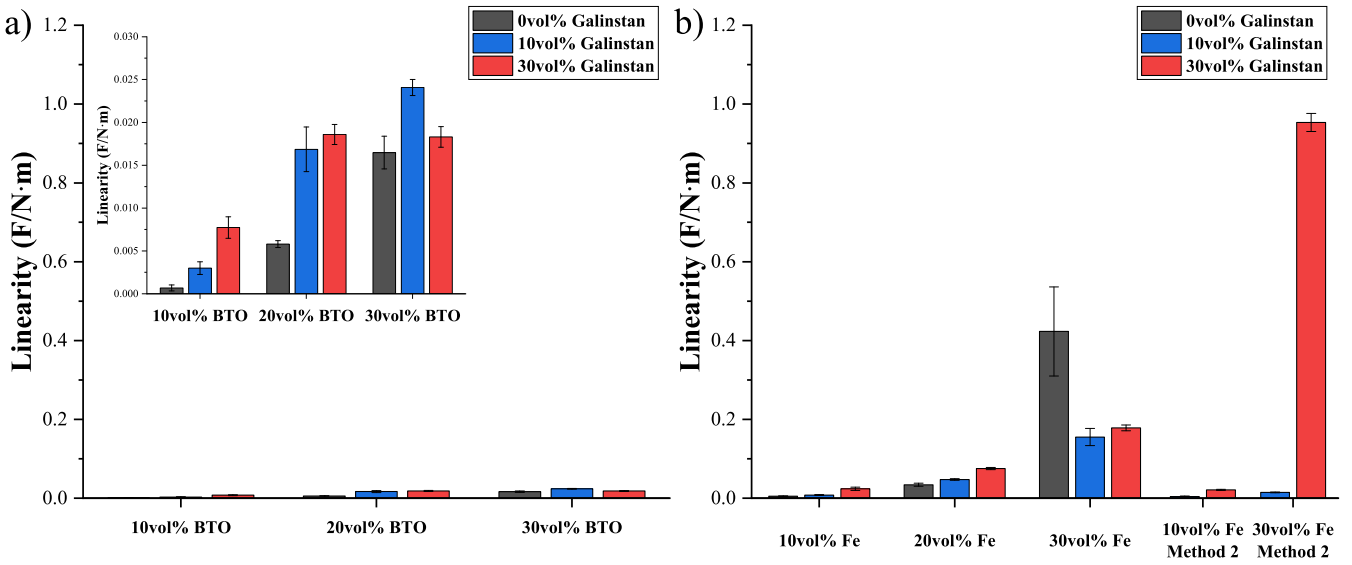

Figure 10. Permittivity dependence on compression, termed "linearity", of the multimaterial composites at varying concentrations of (a) barium titanate and (b) iron with 0, 10, and 30 vol % of galinstan.

permittivity reduction from roughly 8 to 4.5 in carbon black-filled rubber.[63] The permittivity reduction in these composites is ascribed to reorientation of anisotropic fillers and the breaking of the conductive network, respectively, not directly to a change in polarizability of the polymer.

Neither of these explanations satisfactorily explain the effect of deformation on liquid metal multimaterial composites, as seen in Figure 10. Neither Fe nor BTO forms conductive chains or paths in the composite (as demonstrated by low dielectric loss for most samples), and all fillers are assumed to be isotropic on average. For all composites measured, compression caused an increase in permittivity (displayed as "linearity" in units of F/N m). This is in line with previously published results with bulk elastomers, as while tensile deformation causes uncoiling of polymer chains, compressive strain is expected to have the opposite effect. For BTO–GaInSn composites, increasing the filler concentration generally increased the change in permittivity with the compressive load. This change was not independent of composite composition. 20BTO had a linearity of 5.8×10^{-3} F/N m, while 10BTO 10GaInSn had a linearity of 3.0×10^{-3} F/N m (both composites having 20% filler). Similarly, 30BTO 10GaInSn had a linearity of 2.4×10^{-2} F/N m, while 10BTO 30GaInSn had a linearity of 7.7×10^{-3} F/N m (both composites having 40% filler). These comparisons suggest that galinstan suppresses the effect of compression on permittivity.

The same effect is seen with Fe composites (both FM1 and FM2) as 20Fe and 30Fe 10GaInSn show higher changes in permittivity with load as compared to 10Fe 10GaInSn and 10Fe 30GaInSn. This may suggest that rigid fillers exert extra stress on the encapsulating polymer, which influences polarizability, whereas galinstan, as a liquid, deformable filler, mitigates some of the force exerted on the PDMS. Changes in permittivity on the rigid fillers themselves should be negligible with compression in the force range measured. A similar effect is seen in dispersions of neat galinstan with slightly higher linearity values than corresponding neat BTO composites and slightly lower than the neat Fe composites (linearity of neat 10 vol % GaInSn was 2.3×10^{-3} F/N m). As the increase in galinstan concentration did not consistently reduce composite compressive modulus, it is unlikely that this effect is solely due to a reduction in stress between the PDMS and the galinstan. Rather, it is likely that the galinstan reduces interactions between the rigid particles and the polymer. This is highlighted by the comparison between Fe–FM1 and Fe–FM2 composites. For 30Fe, the addition of galinstan reduced the change in permittivity with compression when FM1 was used. In this case, galinstan and iron are aggregated and the interaction between PDMS and iron is mitigated by the galinstan. For FM2, galinstan and iron are discrete and the addition of galinstan increases the change in permittivity with compression due to an additive effect of the two fillers. Increases in change in permittivity with compression were seen for 10Fe as well, but the differences were minimal as the linearity is also comparatively small.

5. CONCLUSIONS

In the work presented here, multimaterial composites of galinstan and iron or barium titanate were rigorously evaluated with respect to morphology, mechanical properties, dielectric behavior, and performance as for pressure sensor applications. This work highlights the novelty of utilizing discrete materials to form multimaterial composites that achieve a balance between superior electrical performance and low modulus for pressure sensing applications by balancing and tuning the desirable mechanical and electrical properties. With respect to barium titanate, it was found that GaInSn–BTO composites demonstrated unique mechanical behavior than what would be expected from either filler. Specifically, galinstan's impact on composite modulus and viscosity is different from that expected of a liquid filler (strictly decreasing modulus/viscosity), a rigid filler (significant increase in modulus/viscosity), or an increase in modulus (at sufficiently high concentration). Galinstan did not increase lossy behavior in BTO composites and added to material sensitivity comparably to the ceramic material despite the permittivity being dominated by BTO. However, galinstan did improve the linearity of the composite material as a pressure sensor, making utilization of the composite simpler in future applications. The GaInSn–BTO composite that achieved the desired balance

https://doi.org/10.1021/acsami.1c21734
ACS Appl. Mater. Interfaces XXXX, XXX, XXX–XXX

between a soft material and high permittivity was the 30BTO 10GaInSn composite, as it had one of the highest permittivity and a relatively low modulus with a high sensitivity when used as a pressure sensor. Iron composites were considerably more complex than BTO due to aggregation of galinstan droplets around the iron particles. By analyzing the results of two different fabrication processes, one where the materials are added simultaneously (FM1) and mixed for 2 h and another where the iron is added in the last 10 min of galinstan mixing (FM2), the effect of galinstan−iron adhesion and aggregation was evaluated. For FM1, at low bulk concentrations of the filler, galinstan was able to act as a lubricant or improve stress transfer between the PDMS and the iron, although the iron appeared to impede the full deformation of galinstan and jamming eventually resulted in higher modulus values regardless. Iron composites made using FM2 demonstrated mechanical deformation closer to what was expected from a blend of the two fillers separately. The microcapacitor model was used to effectively understand both sets of composites, particularly, as FM1 composites showed a reduction in the available capacitor electrode due to aggregation. Pressure sensing showed a high degree of dependence on particle aggregation within the composite and a stronger dependence on the rigid filler than galinstan with respect to material linearity. The GaInSn−Fe composite that achieved the highest permittivity and highest sensitivity when used as a pressure sensor was the 30Fe 30GaInSn−FM2 composite; however, it had a much larger modulus than all the other composites. Therefore, the most desired balance for these composites between low modulus and high permittivity for the GaInSn−Fe composites was the 30Fe 30GaInSn−FM1 composite. The improved modulus, permittivity, phase angle behavior, sensitivity, and linearity of composites when using combinations of galinstan and rigid fillers, which are highly dependent on formulation (relative concentrations), suggest that sensing materials with precisely calibrated material properties are highly achievable. By realizing these materials, the current state of the art of inherently stretchable, robust, and highly responsive sensors, circuits, and electronics will be improved and developed for robotics, wearable systems, and other human-facing devices.

■ ASSOCIATED CONTENT

Supporting Information

The Supporting Information is available free of charge at https://pubs.acs.org/doi/10.1021/acsami.1c21734.

SEM and XRD of iron and barium titanate particles, as well as relative permittivity and phase angle as a function of frequency for neat GaInSn composites (PDF)

■ AUTHOR INFORMATION

Corresponding Author

Amanda S. Koh − *Chemical and Biological Engineering Department, University of Alabama, Tuscaloosa, Alabama 35487, United States*; Email: askoh@eng.ua.edu

Author

Elizabeth Bury − *Chemical and Biological Engineering Department, University of Alabama, Tuscaloosa, Alabama 35487, United States*; orcid.org/0000-0003-3879-0522

Complete contact information is available at: https://pubs.acs.org/10.1021/acsami.1c21734

Author Contributions

The manuscript was written through contributions of all authors. All authors have given approval to the final version of the manuscript.

Funding

NSF Graduate Research Fellowships Program (GRFP) #2021323649.

Notes

The authors declare no competing financial interest.

■ ACKNOWLEDGMENTS

The authors would like to acknowledge the University of Alabama Chemical Engineering Department and the NSF Graduate Research Fellowships Program (GRFP) for financial support. The authors also wish to acknowledge the UA Analytical Research Center for instrumental and technical support.

■ REFERENCES

(1) Qi, D.; Zhang, K.; Tian, G.; Jiang, B.; Huang, Y. Stretchable Electronics Based on PDMS Substrates. *Adv. Mater.* **2021**, *33*, 2003155.

(2) Larmagnac, A.; Eggenberger, S.; Janossy, H.; Vörös, J. Stretchable electronics based on Ag-PDMS composites. *Sci. Rep.* **2014**, *4*, 7254.

(3) Miao, L.; Guo, H.; Wan, J.; Wang, H.; Song, Y.; Chen, H.; Chen, X.; Zhang, H. Localized modulus-controlled PDMS substrate for 2D and 3D stretchable electronics. *J. Micromech. Microeng.* **2020**, *30*, 045001.

(4) Forró, C.; Ihle, S. J.; Reichmuth, A. M.; Han, H.; Stauffer, F.; Weaver, S.; Bonnin, A.; Stampanoni, M.; Tybrandt, K.; Vörös, J. Visualizing and Analyzing 3D Metal Nanowire Networks for Stretchable Electronics. *Adv. Theory Simul.* **2020**, *3*, 2000038.

(5) Kong, K. T. S.; Mariatti, M.; Rashid, A. A.; Busfield, J. J. C. Enhanced conductivity behavior of polydimethylsiloxane (PDMS) hybrid composites containing exfoliated graphite nanoplatelets and carbon nanotubes. *Composites, Part B* **2014**, *58*, 457−462.

(6) Sim, K.; Rao, Z.; Ershad, F.; Yu, C. Rubbery Electronics Fully Made of Stretchable Elastomeric Electronic Materials. *Adv. Mater.* **2020**, *32*, 1902417.

(7) Chua, T. P.; Mariatti, M.; Azizan, A.; Rashid, A. A. Effects of surface-functionalized multi-walled carbon nanotubes on the properties of poly(dimethyl siloxane) nanocomposites. *Compos. Sci. Technol.* **2010**, *70*, 671−677.

(8) Mutiso, R. M.; Winey, K. I. Electrical Conductivity of Polymer Nanocomposites. In *Polymer Science: A Comprehensive Reference*; Matyjaszewski, K., Möller, M., Eds.; Elsevier: Amsterdam, 2012; pp 327−344.

(9) Beena, P.; Jayanna, H. Dielectric studies and AC conductivity of piezoelectric barium titanate ceramic polymer composites. *Polym. Polym. Compos.* **2019**, *27*, 619−625.

(10) Goyal, R. K.; Katkade, S. S.; Mule, D. M. Dielectric, mechanical and thermal properties of polymer/BaTiO3 composites for embedded capacitor. *Composites, Part B* **2013**, *44*, 128−132.

(11) Cai, L.; Zhang, S.; Miao, J.; Yu, Z.; Wang, C. Fully Printed Stretchable Thin-Film Transistors and Integrated Logic Circuits. *ACS Nano* **2016**, *10*, 11459−11468.

(12) Psarras, G. C.; Manolakaki, E.; Tsangaris, G. M. Dielectric dispersion and ac conductivity in—Iron particles loaded—polymer composites. *Composites, Part A* **2003**, *34*, 1187−1198.

(13) Zois, H.; Apekis, L.; Mamunya, Y. P. Dielectric properties and morphology of polymer composites filled with dispersed iron. *J. Appl. Polym. Sci.* **2003**, *88*, 3013−3020.

(14) Baker, C.; Ismat Shah, S.; Hasanain, S. K. Magnetic behavior of iron and iron-oxide nanoparticle/polymer composites. *J. Magn. Magn. Mater.* **2004**, *280*, 412−418.

(15) Cho, J.; Joshi, M. S.; Sun, C. T. Effect of inclusion size on mechanical properties of polymeric composites with micro and nano particles. *Compos. Sci. Technol.* **2006**, *66*, 1941−1952.
(16) Fu, S.-Y.; Feng, X.-Q.; Lauke, B.; Mai, Y.-W. Effects of particle size, particle/matrix interface adhesion and particle loading on mechanical properties of particulate−polymer composites. *Composites, Part B* **2008**, *39*, 933−961.
(17) Gallone, G.; Carpi, F.; De Rossi, D.; Levita, G.; Marchetti, A. Dielectric constant enhancement in a silicone elastomer filled with lead magnesium niobate−lead titanate. *Mater. Sci. Eng., C* **2007**, *27*, 110−116.
(18) Díez-Pascual, A. M.; Ashrafi, B.; Naffakh, M.; González-Domínguez, J. M.; Johnston, A.; Simard, B.; Martínez, M. T.; Gómez-Fatou, M. A. Influence of carbon nanotubes on the thermal, electrical and mechanical properties of poly(ether ether ketone)/glass fiber laminates. *Carbon* **2011**, *49*, 2817−2833.
(19) Dickey, M. D. Stretchable and Soft Electronics using Liquid Metals. *Adv. Mater.* **2017**, *29*, 1606425.
(20) Lin, Y.; Genzer, J.; Dickey, M. D. Attributes, Fabrication, and Applications of Gallium-Based Liquid Metal Particles. *Adv. Sci.* **2020**, *7*, 2000192.
(21) Wu, H.; Zhang, L.; Jiang, S.; Zhang, Y.; Zhang, Y.; Xin, C.; Ji, S.; Zhu, W.; Li, J.; Hu, Y.; Wu, D.; Chu, J. Ultrathin and High-Stress-Resolution Liquid-Metal-Based Pressure Sensors with Simple Device Structures. *ACS Appl. Mater. Interfaces* **2020**, *12*, 55390−55398.
(22) Majidi, C.; Kramer, R.; Wood, R. J. A non-differential elastomer curvature sensor for softer-than-skin electronics. *Smart Mater. Struct.* **2011**, *20*, 105017.
(23) Neumann, T. V.; Dickey, M. D. Liquid Metal Direct Write and 3D Printing: A Review. *Adv. Mater. Technol.* **2020**, *5*, 2000070.
(24) Park, Y.-L.; Majidi, C.; Kramer, R.; Bérard, P.; Wood, R. J. Hyperelastic pressure sensing with a liquid-embedded elastomer. *J. Micromech. Microeng.* **2010**, *20*, 125029.
(25) Bartlett, M. D.; Fassler, A.; Kazem, N.; Markvicka, E. J.; Mandal, P.; Majidi, C. Stretchable, high-k dielectric elastomers through liquid-metal inclusions. *Adv. Mater.* **2016**, *28*, 3726−3731.
(26) Koh, A.; Sietins, J.; Slipher, G.; Mrozek, R. Deformable liquid metal polymer composites with tunable electronic and mechanical properties. *J. Mater. Res.* **2018**, *33*, 2443−2453.
(27) Wang, Q.; Yu, Y.; Liu, J. Preparations, Characteristics and Applications of the Functional Liquid Metal Materials. *Adv. Eng. Mater.* **2018**, *20*, 1700781.
(28) Daalkhaijav, U.; Yirmibesoglu, O. D.; Walker, S.; Mengüç, Y. Rheological Modification of Liquid Metal for Additive Manufacturing of Stretchable Electronics. *Adv. Mater. Technol.* **2018**, *3*, 1700351.
(29) Yao, S.-H.; Dang, Z.-M.; Jiang, M.-J.; Bai, J. BaTiO3-carbon nanotube/polyvinylidene fluoride three-phase composites with high dielectric constant and low dielectric loss. *Appl. Phys. Lett.* **2008**, *93*, 182905.
(30) Carpi, F.; Migliore, A.; Serra, G.; Rossi, D. D. Helical dielectric elastomer actuators. *Smart Mater. Struct.* **2005**, *14*, 1210−1216.
(31) Conley, G. M.; Aebischer, P.; Nöjd, S.; Schurtenberger, P.; Scheffold, F. Jamming and overpacking fuzzy microgels: Deformation, interpenetration, and compression. *Sci. Adv.* **2017**, *3*, No. e1700969.
(32) Foudazi, R.; Masalova, I.; Malkin, A. Y. The role of interdroplet interaction in the physics of highly concentrated emulsions. *Colloid J.* **2010**, *72*, 74−92.
(33) Princen, H. M. Rheology of foams and highly concentrated emulsions: I. Elastic properties and yield stress of a cylindrical model system. *J. Colloid Interface Sci.* **1983**, *91*, 160−175.
(34) Xie, J.; Wang, Y.; Dong, R.; Tao, K. Wearable Device Oriented Flexible and Stretchable Energy Harvester Based on Embedded Liquid-Metal Electrodes and FEP Electret Film. *Sensors* **2020**, *20*, 458.
(35) Guo, S.; Wang, P.; Zhang, J.; Luan, W.; Xia, Z.; Cao, L.; He, Z. Flexible liquid metal coil prepared for electromagnetic energy harvesting and wireless charging. *Front. Energy* **2019**, *13*, 474−482.
(36) Li, G.; Lee, D.-W. An advanced selective liquid-metal plating technique for stretchable biosensor applications. *Lab Chip* **2017**, *17*, 3415−3421.
(37) Liu, D.; Su, L.; Liao, J.; Reeja-Jayan, B.; Majidi, C. Rechargeable Soft-Matter EGaIn-MnO2 Battery for Stretchable Electronics. *Adv. Energy Mater.* **2019**, *9*, 1902798.
(38) Bury, E.; Chun, S.; Koh, A. S. Recent Advances in Deformable Circuit Components with Liquid Metal. *Adv. Electron. Mater.* **2021**, *7*, 2001006.
(39) Sharma, S.; Chhetry, A.; Sharifuzzaman, M.; Yoon, H.; Park, J. Y. Wearable Capacitive Pressure Sensor Based on MXene Composite Nanofibrous Scaffolds for Reliable Human Physiological Signal Acquisition. *ACS Appl. Mater. Interfaces* **2020**, *12*, 22212−22224.
(40) Cheng, Y.; Wang, R.; Sun, J.; Gao, L. A Stretchable and Highly Sensitive Graphene-Based Fiber for Sensing Tensile Strain, Bending, and Torsion. *Adv. Mater.* **2015**, *27*, 7365−7371.
(41) Panda, S.; Acharya, B. PDMS/MWCNT nanocomposites as capacitive pressure sensor and electromagnetic interference shielding materials. *J. Mater. Sci.: Mater. Electron.* **2021**, *32*, 16215−16229.
(42) Ko, Y.; Yoon, H.; Kwon, S.; Lee, H.; Park, M.; Jeon, I.; Lim, J. A.; Chung, S.; Lee, S.-S.; Sung, B. J.; Kim, J.-H.; Kim, H. Elastomeric high-κ composites of low dielectric loss tangent: Experiment and simulation. *Composites, Part B* **2020**, *201*, 108337.
(43) Zhu, L.; Wang, B.; Handschuh-Wang, S.; Zhou, X. Liquid Metal−Based Soft Microfluidics. *Small* **2020**, *16*, 1903841.
(44) Jiang, L.; Betts, A.; Kennedy, D.; Jerrams, S. The fabrication of dielectric elastomers from silicone rubber and barium titanate: employing equi-biaxial pre-stretch to achieve large deformations. *J. Mater. Sci.* **2015**, *50*, 7930−7938.
(45) Cholleti, E. R.; Stringer, J.; Kelly, P.; Bowen, C.; Aw, K. Mechanical Behaviour of Large Strain Capacitive Sensor with Barium Titanate Ecoflex Composite Used to Detect Human Motion. *Robotics* **2021**, *10*, 69.
(46) Shivashankar, H.; Sangamesh, R.; Kulkarni, S. Processing and investigation of mechanical characteristics on the polydimethylsiloxane/carbon black composites. *Mater. Res. Express* **2019**, *6*, 105340.
(47) Dimiev, A.; Zakhidov, D.; Genorio, B.; Oladimeji, K.; Crowgey, B.; Kempel, L.; Rothwell, E. J.; Tour, J. M. Permittivity of Dielectric Composite Materials Comprising Graphene Nanoribbons. The Effect of Nanostructure. *ACS Appl. Mater. Interfaces* **2013**, *5*, 7567−7573.
(48) Zhang, G.; Li, Q.; Allahyarov, E.; Li, Y.; Zhu, L. Challenges and Opportunities of Polymer Nanodielectrics for Capacitive Energy Storage. *ACS Appl. Mater. Interfaces* **2021**, *13*, 37939−37960.
(49) Matsumoto, M.; Miyata, Y. Complex permittivity based on equivalent circuit model for polymer/metal composite. Frequency dependence of permittivity as function of concentration. *IEEE Trans. Dielectr. Electr. Insul.* **1999**, *6*, 27−34.
(50) Dang, Z.-M.; Peng, B.; Xie, D.; Yao, S.-H.; Jiang, M.-J.; Bai, J. High dielectric permittivity silver/polyimide composite films with excellent thermal stability. *Appl. Phys. Lett.* **2008**, *92*, 112910.
(51) Ogitani, S.; Bidstrup-Allen, S. A.; Kohl, P. A. Factors influencing the permittivity of polymer/ceramic composites for embedded capacitors. *IEEE Trans. Adv. Packag.* **2000**, *23*, 313−322.
(52) Dang, Z.-M.; Zha, J.-W.; Yu, Y.; Zhou, T.; Song, H.-T.; Li, S.-T. Microstructure and dielectric characterization of micro- nanosize co-filled composite films with high dielectric permittivity. *IEEE Trans. Dielectr. Electr. Insul.* **2011**, *18*, 1518−1525.
(53) Yun, G.; Tang, S.-Y.; Sun, S.; Yuan, D.; Zhao, Q.; Deng, L.; Yan, S.; Du, H.; Dickey, M. D.; Li, W. Liquid metal-filled magnetorheological elastomer with positive piezoconductivity. *Nat. Commun.* **2019**, *10*, 1300.
(54) Zhang, Z.; Tang, L.; Chen, C.; Yu, H.; Bai, H.; Wang, L.; Qin, M.; Feng, Y.; Feng, W. Liquid metal-created macroporous composite hydrogels with self-healing ability and multiple sensations as artificial flexible sensors. *J. Mater. Chem. A* **2021**, *9*, 875−883.
(55) Ali, M. M.; Narakathu, B. B.; Emamian, S.; Chlaihawi, A. A.; Aljanabi, F.; Maddipatla, D.; Bazuin, B. J.; Atashbar, M. Z. Eutectic Ga-In liquid metal based flexible capacitive pressure sensor. *2016 IEEE Sensors, Oct 30−Nov 3, 2016*, 2016; pp 1−3.
(56) Ali, S.; Maddipatla, D.; Narakathu, B. B.; Chlaihawi, A. A.; Emamian, S.; Janabi, F.; Bazuin, B. J.; Atashbar, M. Z. Flexible

https://doi.org/10.1021/acsami.1c21734
ACS Appl. Mater. Interfaces XXXX, XXX, XXX−XXX

Capacitive Pressure Sensor Based on PDMS Substrate and Ga−In Liquid Metal. *IEEE Sens. J.* **2019**, *19*, 97−104.
(57) Pan, C.; Markvicka, E. J.; Malakooti, M. H.; Yan, J.; Hu, L.; Matyjaszewski, K.; Majidi, C. A Liquid-Metal−Elastomer Nanocomposite for Stretchable Dielectric Materials. *Adv. Mater.* **2019**, *31*, 1900663.
(58) Tutika, R.; Kmiec, S.; Haque, A. B. M. T.; Martin, S. W.; Bartlett, M. D. Liquid Metal−Elastomer Soft Composites with Independently Controllable and Highly Tunable Droplet Size and Volume Loading. *ACS Appl. Mater. Interfaces* **2019**, *11*, 17873−17883.
(59) Yang, J.; Tang, D.; Ao, J.; Ghosh, T.; Neumann, T. V.; Zhang, D.; Piskarev, Y.; Yu, T.; Truong, V. K.; Xie, K.; Lai, Y. C.; Li, Y.; Dickey, M. D. Ultrasoft Liquid Metal Elastomer Foams with Positive and Negative Piezopermittivity for Tactile Sensing. *Adv. Funct. Mater.* **2020**, *30*, 2002611.
(60) Kumar, A.; Patra, K. Proposal of a generic constitutive model for deformation-dependent dielectric constant of dielectric elastomers. *Eng. Sci. Technol., Int. J.* **2021**, *24*, 1347.
(61) Cohen, N.; Oren, S. S.; deBotton, G. The evolution of the dielectric constant in various polymers subjected to uniaxial stretch. *Extreme Mech. Lett.* **2017**, *16*, 1−5.
(62) Fujihara, R.; Kurimoto, M.; Naya, K.; Kato, T.; Imanaka, M.; Sugimoto, S.; Suzuoki, Y. Effect of Filler Amount on Relative Permittivity and Deformation Rate of TiO_2/Silicone Elastomer Composite. *2019 IEEE Conference on Electrical Insulation and Dielectric Phenomena (CEIDP), Oct 20−23, 2019*, 2019; pp 466−469.
(63) Huang, Y.; Schadler, L. S. Understanding the strain-dependent dielectric behavior of carbon black reinforced natural rubber − An interfacial or bulk phenomenon? *Compos. Sci. Technol.* **2017**, *142*, 91−97.

https://doi.org/10.1021/acsami.1c21734
ACS Appl. Mater. Interfaces XXXX, XXX, XXX−XXX